

# Resolving Geometric Excitations of Fractional Quantum Hall States

Yang Liu,<sup>1,2</sup> Tongzhou Zhao,<sup>1</sup> and T. Xiang<sup>1,2,\*</sup>

<sup>1</sup>*Beijing National Laboratory for Condensed Matter Physics and Institute of Physics,  
Chinese Academy of Sciences, Beijing 100190, China.*

<sup>2</sup>*School of Physical Sciences, University of Chinese Academy of Sciences, Beijing 100049, China.*

The quantum dynamics of the intrinsic metric profoundly influence the neutral excitations in the fractional quantum Hall system, as established by Haldane in 2011 [1], and further evidenced by a recent two-photon experiment [2]. Despite these advancements, a comprehensive understanding of the dynamic properties of these excitations, especially at long wavelengths, continues to elude interest. In this study, we employ tensor-network methods to investigate the neutral excitations of the Laughlin and Moore-Read states on an infinite cylinder. This investigation deepens our understanding of the excitation spectrum in regions where traditional methods do not work effectively. The spectral functions for both states reveal the presence of  $S = -2$  geometric excitations. For the first time, we unveil the complex spectra of both neutral fermion and bosonic Girvin-MacDonald-Platzman modes within the excitation continuum by calculating the three-particle density response function for the Moore-Read state. Our findings support the hypothesis of emergent supersymmetry and highlight the potential for detecting neutral fermions in future experiments.

*Introduction* — Neutral excitations in the fractional quantum Hall effect (FQHE) have drawn intensive attention over the past decades. The pioneering work by Girvin, MacDonald and Platzman (GMP) [3, 4] interprets the neutral excitation in the Laughlin state [5] as a collective density fluctuation mode, analogous to the roton excitation in superfluid helium [6–9]. The energy minimum of GMP mode, known as the magnetoroton or bosonic exciton, has been confirmed by several experiments [10–13]. Haldane proposed a geometric interpretation of this mode, suggesting that the fluctuation of the intrinsic metric determines its dynamics in the long-wavelength limit [1, 14, 15]. Perturbations on the metric introduce a new excitation in the d-wave channel, possessing both chirality and topological order [16–26], which was observed through circularly polarized resonant inelastic light scattering [2].

The Moore-Read (MR) state [27–29] involves the pairing of composite fermions [30], resulting in two types of excitations depending on the electron number: a magnetoroton appears when the electron number is even (even parity), while a neutral fermion emerges when the electron number is odd (odd parity), confirmed by the exact diagonalization [31–33]. Unlike the magnetoroton, a neutral fermion carries a half-integer angular momentum [34]. The edge states corresponding to the neutral fermions possess non-Abelian statistics. Through quantum interference, they have great potential in the application of topological quantum computing [35–38].

Recent studies indicate that both types of excitations can be integrated into a cohesive theory if identified as superpartners of an emergent supersymmetry [39] that can be detected from its bulk or edge excitations [40, 41]. For the MR state, the two bulk excitations correspond to two edge states known as the chiral charge boson and the copropagating Majorana fermion, associated with  $\mathcal{N} = (1, 0)$  supersymmetry in  $(1 + 1)$  dimensions [42, 43].

According to this theory, these excitations should merge in the long-wavelength limit as a manifestation of supersymmetry. However, due to finite size constraints, achieving this limit is challenging with exact diagonalization or other numerical methods.

In this study, we calculate the dynamical spectral functions of the FQHE states on an infinite cylinder using the matrix product state (MPS) renormalization group under the single-mode approximation [44]. Our results demonstrate that MPS can accurately capture the bosonic magnetoroton and neutral fermion excitations in the continuum, providing more detailed information than the GMP ansatz, which only describes the lowest excitation. Moreover, we find that the neutral GMP mode in the long-wavelength limit is a  $S = -2$  geometric excitation (also called a graviton in the literature [45–50]).

*Model and method* — Let us consider a two-dimensional electron gas confined to the lowest Landau level on an infinite cylinder along the x-axis with circumference  $L_y$ . The parent Hamiltonian of the Laughlin state in the Landau gauge is defined by a two-body interaction

$$H_L = \sum_k V_k \rho_k \rho_{-k}, \quad (1)$$

where  $V_k$  is the Fourier transform of a projected pseudopotential [51, 52].  $k = (k_x, k_y)$  is the momentum of electron with  $k_y = n e_y$  ( $n$  an integer) and  $e_y = 2\pi/L_y$ .  $k_x$  is continuous on an infinite cylinder.  $\rho_k$  is the projected density operator defined in terms of the electron operator  $c_n$  in the orbital basis space as

$$\rho_{k_x, m e_y} = \sum_n e^{i \tilde{k}_x (2n+m)/2} c_n^\dagger c_{n+m}, \quad (2)$$

where  $\tilde{k}_x = k_x e_y$ .

Similarly, the parent Hamiltonian of the MR state is



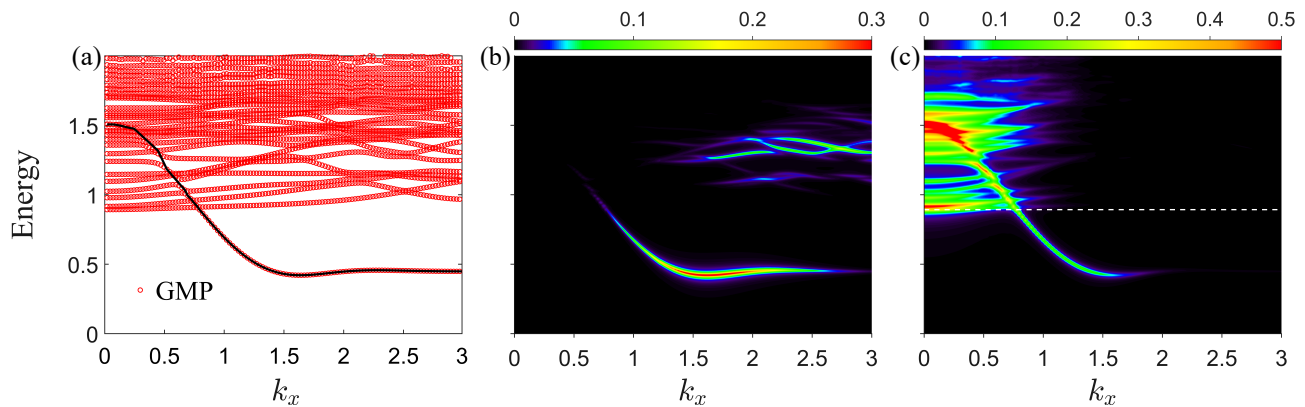


FIG. 2. (a) The energy dispersions of the excited states for the  $\nu = 1/3$  Laughlin state on an infinite cylinder with  $L_y = 18$  along the momentum line  $k = (k_x, 0)$ , obtained with an MPS bond dimension  $D = 88$ , (b) single-particle density spectra and (c) pairing density spectra of  $O^-$ . The white dashed lines in (c) represent the lower bound of the excitation continuum. The black line in (a) depicts the energy dispersion of the GMP mode corresponding to the excitation with the highest spectral weight at  $(k = 0, E = 1.5)$  in (c).

impurity tensor  $B_i$  multiplied by a site-dependent phase factor. For example, for a  $M = 2$  system,  $B$  is defined as

$$\text{---} \bigcirc \text{---} = \text{---} \bigcirc \text{---} \bigcirc \text{---} + e^{i\tilde{k}_x} \text{---} \bigcirc \text{---} \bigcirc \text{---}. \quad (10)$$

*Spectral functions* — Upon determining all the local tensors variationally, we can use the eigenvalues and eigenfunctions of the ground and excited states to evaluate the spectral function of a physical variable  $O_k$

$$I(\omega, k) = \sum_n |\langle \Phi_{k,n}(B) | O_k | \Psi(A) \rangle|^2 \delta(\hbar\omega - E_n), \quad (11)$$

where  $E_n$  is the  $n$ th eigenvalue of the excited state and  $\Phi_{k,n}$  the corresponding eigenfunction.

In the  $\nu = 1/3$  Laughlin state, the lowest collective excitations are the bosonic GMP modes. The GMP mode essentially represents a quantized wave of charge density propagating through the electron system, detectable by the single-particle density spectral function of  $O_k = \delta\rho_k$ . As shown in Fig. 2(a-b), the dispersion of this GMP mode becomes flat in the large  $k$  limit. The spectrum shows a distinct magnetoroton minimum at  $k \approx 1.7$  with an energy  $E = 0.41$ , indicating a softening of this mode at a specific length scale. At small  $k$ , the GMP mode merges into the continuum of excitations, and its spectral weight diminishes significantly, primarily due to the quartic dependence of  $S(k)$  on  $k$ .

The single-particle density spectrum also reveals pronounced features of charge-neutral excitations, known as excitons, in the high-energy continuum, with momentum  $k$  ranging from 2 to 3 and energy  $E$  from 1.25 to 1.4. These features likely arise from the excitation of composite fermions to higher effective Landau levels in the composite fermion theory [71–73]. This finding aligns with earlier calculations [74] and is consistent with inelastic photon measurement results [75].

In this Laughlin state, the intrinsic metric associated with GMP couples directly with the two-particle density operators in the long wavelength limit. Thus, to reveal the GMP mode in the continuum, we calculate the pair density spectrum Eq. (11) with  $O_k$  defined by

$$O_k^\pm = \sum_{k_1+k_2=k} k_1^\pm k_2^\pm e^{-(k_1^2+k_2^2)/4} \delta\rho_{k_1} \delta\rho_{k_2}, \quad (12)$$

where  $k^\pm = k_x \pm ik_y$ , corresponding to the  $S = 2$  and  $S = -2$  representations, respectively. We also evaluate the dynamical spectra of other d-wave operators  $O_{x^2-y^2} = O^+ + O^-$  and  $O_{xy} = O^+ - O^-$ . The calculation reveals that only the  $S = -2$  mode contributes to the long-wavelength GMP spectra in the continuum. More specifically, the  $S = -2$  spectrum shows a strong signal at  $k = 0$  and  $E \approx 1.5$ , as depicted in Fig. 2(c), consistent with the exact diagonalization results [21].

At  $k = 0$ , the  $S = -2$  spectrum also reveals a peak just above the lower edge of the continuum at  $E = 0.9$ . This peak corresponds to a bi-roton bound state, where two rotons interact by dipole-dipole interaction to form a bound state with an energy lower than the GMP mode in the continuum [76–78]. However, this bound state does not possess the chirality characteristic of the geometric mode.

Next, we turn to the excitations of the MR state. In the MR state, electrons pair up in a p-wave superconducting-like manner. In addition to the GMP modes, neutral fermion modes emerge in this state. These modes can be described by Majorana fermions bound to vortex excitations in the p-wave paired state.

Based on the calculations of single and three-particle density spectra, we identify two types of excitations, as shown in Fig. 3(a-b). The first type is the bosonic GMP modes, which exhibit energy dispersions similar to those in the Laughlin states. The second type is the neutral

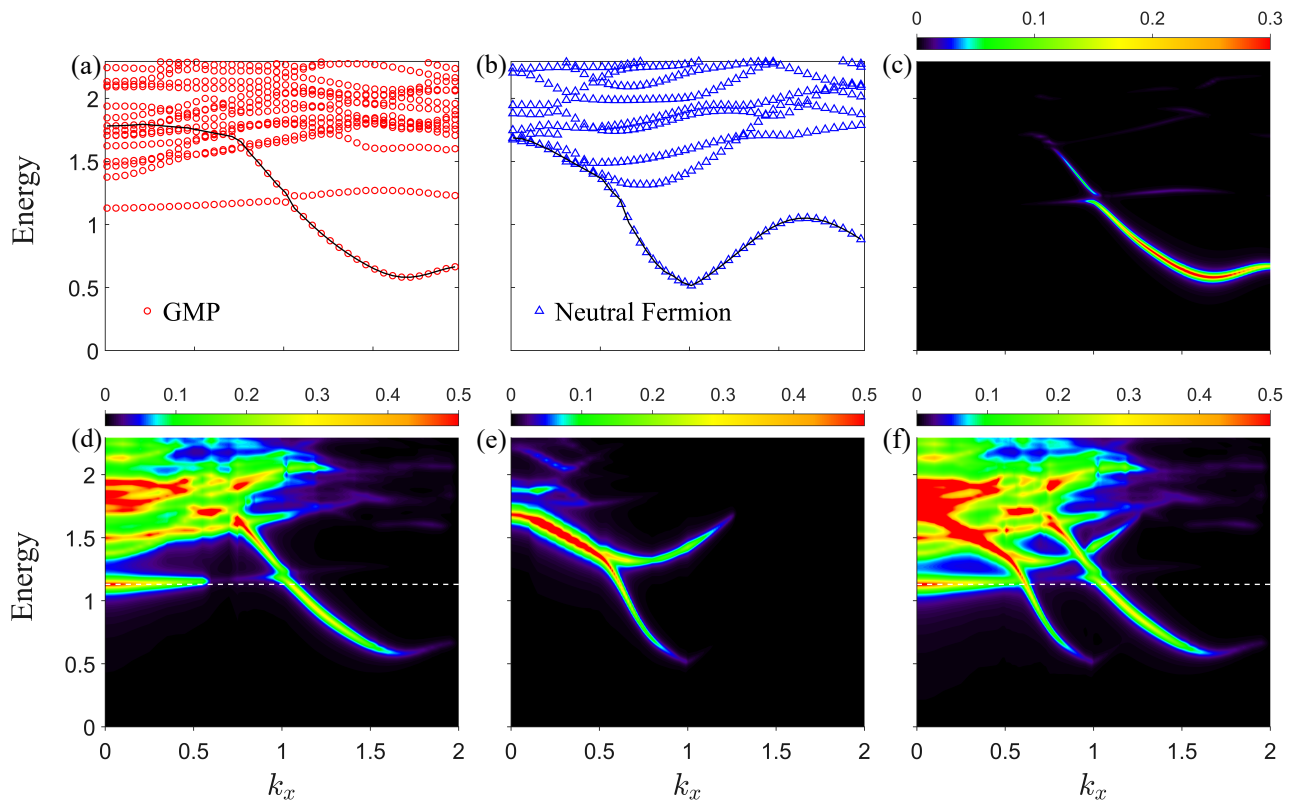


FIG. 3. Energy dispersions, single and three-particle density spectra of the  $\nu = 1/2$  MR state on an infinite cylinder with  $L_y = 16$ , obtained along the momentum points  $k = (k_x, 0)$  under the single-mode approximation of MPS with  $D = 103$ . Energy dispersions of the excited states in (a) the even- and (b) odd-parity sectors. (c) is the single particle density spectra. (d) and (e) are the three-particle density spectra of  $O^-$  in the even- and odd-parity sectors, respectively. (f) is the combined three-particle density spectra of (d) and (e). The black curve in (a) is a guiding line that traces the high-intensity points in the small  $k$  region with the magnetoroton mode shown in (c) and (d) in the large  $k$  region. The black curve in (b) is the energy dispersion of the lowest excited states in the odd-parity MR state. The thin white dashed lines in (d) and (f) are the lower edge of the excitation continuum.

fermion modes, which features a distinct local minimum at  $k_x = 1$ . Our results are consistent with previous finite-system calculations based on the bipartite composite fermions, Jack Polynomials, symmetrization constructions on multilayer systems, and supersymmetric wave functions [79–82].

The single-particle density spectrum, depicted in Fig. 3(c), shows similar results to those in the Laughlin state (see Fig. 2(a)). Notably, the low-energy magnetoroton excitation exhibits a prominent peak at  $k_x \approx 1.6$  and  $E = 0.57$ . However, the spectrum becomes heavily damped upon entering the two-particle excitation continuum. Like the Laughing state, it shows no spectral weight for the GMP modes in the long-wavelength limit.

Unlike in the Laughlin state, the GMP mode does not display a sizable weight in the pair density spectra in the long-wavelength limit due to the paired nature of electrons in the MR state. This pairing modifies the geometry and metric that govern the interactions and correlations. Consequently, the GMP modes do not impact the MR state similarly to the Laughlin state, especially

in the pair density channel.

However, the GMP modes respond strongly to the dynamic fluctuation of the three-particle density operator

$$O_k^\pm = \sum_{k_1 k_2 k_3} k_1^\pm (k_2^\pm + k_3^\pm) e^{-(k_1^2 + k_2^2 + k_3^2)/4} \delta \rho_{k_1} \delta \rho_{k_2} \delta \rho_{k_3} \delta_{k_1 + k_2 + k_3, k}. \quad (13)$$

Again,  $O^\pm$  corresponds to the  $S = \pm 2$  state. Figure 3(d) illustrates the GMP spectra acquired in the  $O^-$  channel. Similar to the Laughlin state, there is a distinct GMP response in the small  $k$  region within the continuum. Compared to the  $S = -2$  mode of the Laughlin state, the spectrum of this mode in the MR state is more broadened in the low- $k$  region, consistent with the result presented in Ref. [21].

GMP modes are linked to collective density oscillations, whereas neutral fermion modes are closely associated with the topological excitations of the MR state. To explore the neutral fermion modes, we compute the MR ground state and the corresponding excited states in the odd parity sector. The analysis of response functions

reveals that both the pair and three-particle density spectral functions exhibit distinct peaks of neutral fermions. Figure 3(e) shows the three-particle density spectra in the neutral fermion channel. This is the first time the spectral function of neutral fermions in the small  $k$  limit is obtained. As illustrated by Fig. 3(f), the GMP and neutral fermion modes tend to merge at  $k = 0$ , hinting at an underlying emergent supersymmetry. Furthermore, the energy of the GMP mode is higher than that of the neutral fermion mode in the continuum, consistent with the published result for the two modes obtained by parametrizing the superspace [82].

*Conclusion and discussion*— In summary, we investigate the neutral excitations of the  $\nu = 1/3$  Laughlin state and the  $\nu = 1/2$  MR state under the single-mode approximation of MPS on an infinite cylinder. Our analysis of the Laughlin state pinpoints the magnetoroton minimum and elucidates the long-wavelength GMP mode within the continuum through the pair density spectral function. From the long-wavelength spectra, we confirm that the GMP mode corresponds to the  $S = -2$  geometric excitation.

For the MR state, we have developed the MPS representations for both ground and excited states across even and odd parity sectors. We probe the bosonic GMP and neutral fermion modes in the MR state in the small  $k$  region, inaccessible via exact diagonalization due to the finite-size effects. Our results confirm that these modes are consistent with the previously proposed emergent supersymmetry. Both GMP and neutral fermion modes emerge in the  $O^-$  d-wave channel. This identification of the  $O^-$  channel would facilitate the development of bimetric field theories [46]. It is worth exploring whether incorporating supersymmetry into this field theory might pair these two modes as superpartners. The dynamic spectra we obtain will also contribute to constructing corresponding massive wave equations for these fields.

Our calculation is based on the parent Hamiltonians, which account only for short-range interactions, not the long-range Coulomb interaction. Nevertheless, we believe that our findings still offer significant qualitative insights into the physics underlying FQHE. Our results suggest that the neutral fermion mode might be explored experimentally through multi-photon experiments, providing a new avenue for empirical verification.

*Acknowledgments*— We have implemented the code for the excited spectrum based on ITensor [83]. We thank Songyang Pu, Zlatko Papić, Kun Yang, Ying Hai Wu, and Tong Liu for helpful discussions. We thank J. Haegeman for the instructions on the KrylovKit package. This work is supported by the NSFC grant No. 12488201, and by the China Postdoctoral Science Foundation grant No. 2023M743742.

\* [txiang@iphy.ac.cn](mailto:txiang@iphy.ac.cn)

- [1] F. D. M. Haldane, Geometrical description of the fractional quantum hall effect, *Phys. Rev. Lett.* **107**, 116801 (2011).
- [2] J. Liang, Z. Liu, Z. Yang, Y. Huang, U. Wurstbauer, C. R. Dean, K. W. West, L. N. Pfeiffer, L. Du, and A. Pinczuk, Evidence for chiral graviton modes in fractional quantum hall liquids, *Nature*, 1 (2024).
- [3] S. M. Girvin, A. H. MacDonald, and P. M. Platzman, Collective-excitation gap in the fractional quantum hall effect, *Phys. Rev. Lett.* **54**, 581 (1985).
- [4] S. M. Girvin, A. H. MacDonald, and P. M. Platzman, Magneto-roton theory of collective excitations in the fractional quantum hall effect, *Phys. Rev. B* **33**, 2481 (1986).
- [5] R. B. Laughlin, Anomalous quantum hall effect: An incompressible quantum fluid with fractionally charged excitations, *Phys. Rev. Lett.* **50**, 1395 (1983).
- [6] A. Bijl, J. De Boer, and A. Michels, Properties of liquid helium ii, *Physica* **8**, 655 (1941).
- [7] R. P. Feynman, Atomic theory of the  $\lambda$  transition in helium, *Phys. Rev.* **91**, 1291 (1953).
- [8] R. P. Feynman, Atomic theory of the two-fluid model of liquid helium, *Phys. Rev.* **94**, 262 (1954).
- [9] R. P. Feynman and M. Cohen, Energy spectrum of the excitations in liquid helium, *Phys. Rev.* **102**, 1189 (1956).
- [10] R. R. Du, H. L. Stormer, D. C. Tsui, L. N. Pfeiffer, and K. W. West, Experimental evidence for new particles in the fractional quantum Hall effect, *Phys. Rev. Lett.* **70**, 2944 (1993).
- [11] A. Pinczuk, B. S. Dennis, L. N. Pfeiffer, and K. West, Observation of collective excitations in the fractional quantum hall effect, *Phys. Rev. Lett.* **70**, 3983 (1993).
- [12] M. Kang, A. Pinczuk, B. S. Dennis, L. N. Pfeiffer, and K. W. West, Observation of multiple magnetorotons in the fractional quantum hall effect, *Phys. Rev. Lett.* **86**, 2637 (2001).
- [13] I. V. Kukushkin, J. H. Smet, V. W. Scarola, V. Umansky, and K. von Klitzing, Dispersion of the excitations of fractional quantum hall states, *Science* **324**, 1044 (2009), <https://www.science.org/doi/pdf/10.1126/science.1171472>.
- [14] F. D. M. Haldane, (2009), [arXiv:0906.1854](https://arxiv.org/abs/0906.1854) [cond-mat.str-el].
- [15] F. D. M. Haldane, (2011), [arXiv:1112.0990](https://arxiv.org/abs/1112.0990) [cond-mat.str-el].
- [16] R.-Z. Qiu, F. D. M. Haldane, X. Wan, K. Yang, and S. Yi, Model anisotropic quantum hall states, *Phys. Rev. B* **85**, 115308 (2012).
- [17] B. Yang, Z. Papić, E. H. Rezayi, R. N. Bhatt, and F. D. M. Haldane, Band mass anisotropy and the intrinsic metric of fractional quantum hall systems, *Phys. Rev. B* **85**, 165318 (2012).
- [18] K. Yang, Acoustic wave absorption as a probe of dynamical geometrical response of fractional quantum hall liquids, *Phys. Rev. B* **93**, 161302 (2016).
- [19] B. Yang, Z.-X. Hu, C. H. Lee, and Z. Papić, Generalized pseudopotentials for the anisotropic fractional quantum hall effect, *Phys. Rev. Lett.* **118**, 146403 (2017).
- [20] Z. Liu, A. Gromov, and Z. Papić, Geometric quench and nonequilibrium dynamics of fractional quantum hall states, *Phys. Rev. B* **98**, 155140 (2018).
- [21] S.-F. Liou, F. D. M. Haldane, K. Yang, and E. H. Rezayi,

- Chiral gravitons in fractional quantum hall liquids, *Phys. Rev. Lett.* **123**, 146801 (2019).
- [22] K. Yang, M. O. Goerbig, and B. Douçot, Collective excitations of quantum hall states under tilted magnetic field, *Phys. Rev. B* **102**, 045145 (2020).
- [23] Z. Liu, A. C. Balram, Z. Papić, and A. Gromov, Quench dynamics of collective modes in fractional quantum hall bilayers, *Phys. Rev. Lett.* **126**, 076604 (2021).
- [24] D. X. Nguyen and D. T. Son, Probing the spin structure of the fractional quantum hall magnetoroton with polarized raman scattering, *Phys. Rev. Res.* **3**, 023040 (2021).
- [25] D. X. Nguyen, F. D. M. Haldane, E. H. Rezayi, D. T. Son, and K. Yang, Multiple magnetorotons and spectral sum rules in fractional quantum hall systems, *Phys. Rev. Lett.* **128**, 246402 (2022).
- [26] C. Han and Z. Liu, Anisotropy and quench dynamics of quasiholes in fractional quantum hall liquids, *Phys. Rev. B* **105**, 045108 (2022).
- [27] G. Moore and N. Read, Nonabelions in the fractional quantum hall effect, *Nuclear Physics B* **360**, 362 (1991).
- [28] N. Read and E. Rezayi, Beyond paired quantum hall states: Parafermions and incompressible states in the first excited landau level, *Phys. Rev. B* **59**, 8084 (1999).
- [29] N. Read and D. Green, Paired states of fermions in two dimensions with breaking of parity and time-reversal symmetries and the fractional quantum hall effect, *Phys. Rev. B* **61**, 10267 (2000).
- [30] J. K. Jain, Composite-fermion approach for the fractional quantum hall effect, *Phys. Rev. Lett.* **63**, 199 (1989).
- [31] G. Möller, A. Wójs, and N. R. Cooper, Neutral fermion excitations in the moore-read state at filling factor  $\nu = 5/2$ , *Phys. Rev. Lett.* **107**, 036803 (2011).
- [32] P. Bonderson, A. E. Feiguin, and C. Nayak, Numerical calculation of the neutral fermion gap at the  $\nu = 5/2$  fractional quantum hall state, *Phys. Rev. Lett.* **106**, 186802 (2011).
- [33] Z. Papić, F. D. M. Haldane, and E. H. Rezayi, Quantum phase transitions and the  $\nu=5/2$  fractional hall state in wide quantum wells, *Phys. Rev. Lett.* **109**, 266806 (2012).
- [34] M. Greiter, X.-G. Wen, and F. Wilczek, Paired hall state at half filling, *Phys. Rev. Lett.* **66**, 3205 (1991).
- [35] P. Bonderson, Splitting the topological degeneracy of non-abelian anyons, *Phys. Rev. Lett.* **103**, 110403 (2009).
- [36] W. Bishara and C. Nayak, Odd-even crossover in a non-abelian  $\nu = 5/2$  interferometer, *Phys. Rev. B* **80**, 155304 (2009).
- [37] W. Bishara, P. Bonderson, C. Nayak, K. Shtengel, and J. K. Slingerland, Interferometric signature of non-abelian anyons, *Phys. Rev. B* **80**, 155303 (2009).
- [38] B. Rosenow, B. I. Halperin, S. H. Simon, and A. Stern, Exact solution for bulk-edge coupling in the non-abelian  $\nu = 5/2$  quantum hall interferometer, *Phys. Rev. B* **80**, 155305 (2009).
- [39] A. Gromov, E. J. Martinec, and S. Ryu, Collective excitations at filling factor  $5/2$ : The view from superspace, *Phys. Rev. Lett.* **125**, 077601 (2020).
- [40] K. K. W. Ma, R. Wang, and K. Yang, Realization of supersymmetry and its spontaneous breaking in quantum hall edges, *Phys. Rev. Lett.* **126**, 206801 (2021).
- [41] P. Salgado-Rebolledo and G. Palumbo, Nonrelativistic supergeometry in the moore-read fractional quantum hall state, *Phys. Rev. D* **106**, 065020 (2022).
- [42] C. Hull and E. Witten, Supersymmetric sigma models and the heterotic string, *Physics Letters B* **160**, 398 (1985).
- [43] S. Gates Jr, M. T. Grisaru, L. Mezincescu, and P. Townsend, (1, 0) supergravity, *Nuclear Physics B* **286**, 1 (1987).
- [44] R. Chi, Y. Liu, Y. Wan, H.-J. Liao, and T. Xiang, Spin excitation spectra of anisotropic spin-1/2 triangular lattice heisenberg antiferromagnets, *Phys. Rev. Lett.* **129**, 227201 (2022).
- [45] S. Golkar, D. X. Nguyen, and D. T. Son, Spectral sum rules and magneto-roton as emergent graviton in fractional quantum hall effect, *Journal of High Energy Physics* **2016**, 10.1007/jhep01(2016)021 (2016).
- [46] A. Gromov and D. T. Son, Bimetric theory of fractional quantum hall states, *Phys. Rev. X* **7**, 041032 (2017).
- [47] F. D. M. Haldane, E. H. Rezayi, and K. Yang, Graviton chirality and topological order in the half-filled landau level, *Phys. Rev. B* **104**, L121106 (2021).
- [48] A. Kirmani, K. Bull, C.-Y. Hou, V. Saravanan, S. M. Saeed, Z. Papić, A. Rahmani, and P. Ghaemi, Probing geometric excitations of fractional quantum hall states on quantum computers, *Phys. Rev. Lett.* **129**, 056801 (2022).
- [49] D. X. Nguyen, K. Prabhu, A. C. Balram, and A. Gromov, Supergravity model of the haldane-rezayi fractional quantum hall state, *Phys. Rev. B* **107**, 125119 (2023).
- [50] W. Yuzhu and Y. Bo, Geometric fluctuation of conformal hilbert spaces and multiple graviton modes in fractional quantum hall effect, *Nature Communications* **14**, 2317 (2023).
- [51] F. D. M. Haldane, Fractional quantization of the hall effect: A hierarchy of incompressible quantum fluid states, *Phys. Rev. Lett.* **51**, 605 (1983).
- [52] S. A. Trugman and S. Kivelson, Exact results for the fractional quantum Hall effect with general interactions, *Phys. Rev. B* **31**, 5280 (1985).
- [53] See supplemental material for details, .
- [54] B. Estienne, Z. Papić, N. Regnault, and B. A. Bernevig, Matrix product states for trial quantum hall states, *Phys. Rev. B* **87**, 161112 (2013).
- [55] M. P. Zaletel and R. S. K. Mong, Exact matrix product states for quantum hall wave functions, *Phys. Rev. B* **86**, 245305 (2012).
- [56] V. Crépel, B. Estienne, B. A. Bernevig, P. Lecheminant, and N. Regnault, Matrix product state description of halperin states, *Phys. Rev. B* **97**, 165136 (2018).
- [57] B. A. Bernevig and F. D. M. Haldane, Generalized clustering conditions of jack polynomials at negative jack parameter  $\alpha$ , *Phys. Rev. B* **77**, 184502 (2008).
- [58] B. A. Bernevig and F. D. M. Haldane, Model fractional quantum hall states and jack polynomials, *Phys. Rev. Lett.* **100**, 246802 (2008).
- [59] D.-H. Lee and S.-C. Zhang, Collective excitations in the ginzburg-landau theory of the fractional quantum hall effect, *Phys. Rev. Lett.* **66**, 1220 (1991).
- [60] P. Kalinay, P. Markoš, L. Šamaj, and I. Travěnek, The sixth-moment sum rule for the pair correlations of the two-dimensional one-component plasma: Exact result, *Journal of Statistical Physics* **98**, 639 (2000).
- [61] T. Can, M. Laskin, and P. Wiegmann, Fractional quantum hall effect in a curved space: Gravitational anomaly and electromagnetic response, *Phys. Rev. Lett.* **113**, 046803 (2014).
- [62] T. Can, M. Laskin, and P. B. Wiegmann, Geometry of

- quantum hall states: Gravitational anomaly and transport coefficients, *Annals of Physics* **362**, 752 (2015).
- [63] D. X. Nguyen, T. Can, and A. Gromov, Particle-hole duality in the lowest Landau level, *Phys. Rev. Lett.* **118**, 206602 (2017).
- [64] A. Gromov, S. D. Geraedts, and B. Bradlyn, Investigating anisotropic quantum hall states with bimetric geometry, *Phys. Rev. Lett.* **119**, 146602 (2017).
- [65] J. Wang, S. D. Geraedts, E. H. Rezayi, and F. D. M. Haldane, Lattice Monte Carlo for quantum hall states on a torus, *Phys. Rev. B* **99**, 125123 (2019).
- [66] P. Kumar and F. D. M. Haldane, A numerical study of bounds in the correlations of fractional quantum Hall states, *SciPost Phys.* **16**, 117 (2024).
- [67] S. Östlund and S. Rommer, Thermodynamic limit of density matrix renormalization, *Phys. Rev. Lett.* **75**, 3537 (1995).
- [68] S. Rommer and S. Östlund, Class of ansatz wave functions for one-dimensional spin systems and their relation to the density matrix renormalization group, *Phys. Rev. B* **55**, 2164 (1997).
- [69] J. Haegeman, J. I. Cirac, T. J. Osborne, I. Pizorn, H. Verschelde, and F. Verstraete, Time-dependent variational principle for quantum lattices, *Phys. Rev. Lett.* **107**, 070601 (2011).
- [70] J. Haegeman, B. Pirvu, D. J. Weir, J. I. Cirac, T. J. Osborne, H. Verschelde, and F. Verstraete, Variational matrix product ansatz for dispersion relations, *Phys. Rev. B* **85**, 100408 (2012).
- [71] Higher energy modes of fractional quantum hall effect, *J. Phys. Through Comput.* **1**, 8 (2018).
- [72] D. Majumder and S. S. Mandal, Neutral collective modes in spin-polarized fractional quantum hall states at filling factors  $\frac{1}{3}$ ,  $\frac{2}{5}$ ,  $\frac{3}{7}$ , and  $\frac{4}{9}$ , *Phys. Rev. B* **90**, 155310 (2014).
- [73] B. Yang and F. D. M. Haldane, Nature of quasielectrons and the continuum of neutral bulk excitations in Laughlin quantum hall fluids, *Phys. Rev. Lett.* **112**, 026804 (2014).
- [74] P. M. Platzman and S. He, Resonant Raman scattering from mobile electrons in the fractional quantum hall regime, *Phys. Rev. B* **49**, 13674 (1994).
- [75] T. D. Rhone, D. Majumder, B. S. Dennis, C. Hirjibehedin, I. Dujovne, J. G. Groshaus, Y. Gallais, J. K. Jain, S. S. Mandal, A. Pinczuk, L. Pfeiffer, and K. West, Higher-energy composite fermion levels in the fractional quantum hall effect, *Phys. Rev. Lett.* **106**, 096803 (2011).
- [76] P. M. Platzman and S. He, Resonant Raman scattering from magneto-rotons in the fractional quantum hall liquid, *Physica Scripta* **1996**, 167 (1996).
- [77] K. Park and J. K. Jain, Two-roton bound state in the fractional quantum hall effect, *Phys. Rev. Lett.* **84**, 5576 (2000).
- [78] T. K. Ghosh and G. Baskaran, Modeling two-roton bound state formation in the fractional quantum Hall system, *Phys. Rev. Lett.* **87**, 186803 (2001).
- [79] G. J. Sreejith, A. Wójs, and J. K. Jain, Unpaired composite fermion, topological exciton, and zero mode, *Phys. Rev. Lett.* **107**, 136802 (2011).
- [80] B. Yang, Z.-X. Hu, Z. Papić, and F. D. M. Haldane, Model wave functions for the collective modes and the magneto-roton theory of the fractional quantum hall effect, *Phys. Rev. Lett.* **108**, 256807 (2012).
- [81] C. Repellin, T. Neupert, B. A. Bernevig, and N. Regnault, Projective construction of the  $F_k$  Read-Rezayi fractional quantum hall states and their excitations on the torus geometry, *Phys. Rev. B* **92**, 115128 (2015).
- [82] S. Pu, A. C. Balram, M. Fremling, A. Gromov, and Z. Papić, Signatures of supersymmetry in the  $\nu = 5/2$  fractional quantum hall effect, *Phys. Rev. Lett.* **130**, 176501 (2023).
- [83] M. Fishman, S. R. White, and E. M. Stoudenmire, The ITensor Software Library for Tensor Network Calculations, *SciPost Phys. Codebases*, 4 (2022).

# Supplemental Materials: Resolving Geometric Excitations of Fractional Quantum Hall States

Yang Liu,<sup>1,2</sup> Tong Zhou Zhao,<sup>1</sup> and T. Xiang<sup>1,2,\*</sup>

<sup>1</sup>*Beijing National Laboratory for Condensed Matter Physics and Institute of Physics,  
Chinese Academy of Sciences, Beijing 100190, China.*

<sup>2</sup>*School of Physical Sciences, University of Chinese Academy of Sciences, Beijing 100049, China.*

## Appendix A: Parent Hamiltonians of fractional quantum Hall states on a cylinder

In this section, we elucidate the formalism of the fractional quantum Hall effect (FQHE) on a cylinder. While the formalism used in our analysis is conventional, a thorough introduction to these aspects is beneficial, as published articles often omit crucial details. To enhance readability and ensure logical consistency, we will restate some equations previously mentioned in the main text.

The system under consideration is defined on an open cylinder aligned along the  $x$ -direction. The length and circumference of the cylinder are denoted as  $L_x$  and  $L_y$ , respectively. During subsequent infinite tensor network calculations, we take the limit  $L_x \rightarrow \infty$ . We utilize the Landau gauge  $\mathbf{A} = (0, Bx, 0)$  and consider only the orbitals in the lowest Landau level. The  $m$ th single-particle wave function in the lowest Landau level is defined as:

$$\phi_m(x, y) = \frac{1}{\sqrt{\pi^{1/2} L_y}} e^{ime_y l y} e^{-(x-me_y l)^2/2} \quad (\text{A1})$$

where  $e_y = 2\pi/L_y$  and  $l = \sqrt{\hbar c/eB}$  is the magnetic length. In the discussion below, we set below  $l = 1$ . This Landau orbital has well-defined momentum  $k = (k_x, k_y)$  on an infinite cylinder. The momentum along the  $y$ -axis is quantized  $k_y = me_y$ , while that along the  $x$ -axis is continuous.

A generic two-body interaction in the momentum space reads

$$v(r_1 - r_2) = \sum_k v_k e^{ik \cdot (r_1 - r_2)}. \quad (\text{A2})$$

By utilizing the formula

$$\langle \phi_{m_1} \phi_{m_2} | e^{ik \cdot (r_1 - r_2)} | \phi_{n_1} \phi_{n_2} \rangle = \langle \phi_{m_1} | e^{ik \cdot r_1} | \phi_{n_1} \rangle \langle \phi_{m_2} | e^{-ik \cdot r_2} | \phi_{n_2} \rangle, \quad (\text{A3})$$

$$\langle \phi_m | e^{ik \cdot r} | \phi_n \rangle = \delta_{(m-n)e_y, k_y} e^{-\frac{k^2}{4} + i\frac{k_x k_y}{2} + ink_x e_y}, \quad (\text{A4})$$

we can further express this two-body interaction, also called the parent Hamiltonian, as

$$H = \sum_{k_x} \sum_m v_k \left( e^{-\frac{1}{4}k^2} \rho_{k_x, me_y} \right) \left( e^{-\frac{1}{4}k^2} \rho_{-k_x, -me_y} \right) = \sum_k V_k \rho_k \rho_{-k} \quad (\text{A5})$$

where  $\rho_k$  is the projected density operator

$$\rho_k = \rho_{k_x, me_y} = \sum_n \exp \left[ \frac{i\tilde{k}_x (2n + m)}{2} \right] c_n^\dagger c_{n+m}, \quad (\text{A6})$$

$\tilde{k}_x = k_x e_y$ , and  $c_m^\dagger$  the creation operator of electron.  $V_k = [F(k)]^2 v_k$  is the Fourier transform of the projected interaction, and  $F(k) = \exp(-k^2/4)$  is the form factor for the lowest Landau level.

The Fourier transform of the  $V_1$ -Haldane pseudopotential or Trugman-Kivelson real space potential  $\nabla_i^2 \delta^2(r_i - r_j)$  is  $v_k = 1 - k^2$  [1, 2]. It corresponds to the zero energy Laughlin state. Substituting this expression into Eq. (A5), we find the parent Hamiltonian of the Laughlin state to be:

$$H_L = \frac{(2\pi)^{5/2}}{L_y^3} \sum_{j_1 j_2 j_3 j_4} (j_1 - j_2) (j_3 - j_4) e^{-e_y^2 [(j_1 - j_4)^2 + (j_2 - j_3)^2]/2} \delta_{j_1 + j_2, j_3 + j_4} c_{j_1}^\dagger c_{j_2}^\dagger c_{j_3} c_{j_4} \quad (\text{A7})$$

---

\* txiang@iphy.ac.cn



The three-body Hamiltonian for the Moore-Read (MR) state can be similarly derived. The result is

$$H_{\text{MR}} = \sum_{k_1, k_2} V_{k_1, k_2} \rho_{k_1} \rho_{k_2} \rho_{-k_1 - k_2}, \quad (\text{A8})$$

where

$$V_{k_1, k_2} = F(k_1)F(k_2)F(-k_1 - k_2)v(k_1, k_1), \quad (\text{A9})$$

and  $v(k_1, k_1)$  is the Fourier transform of the three-body interaction

$$\nabla_i^4 \nabla_j^2 \delta^2(r_i - r_j) \delta^2(r_j - r_k), \quad (\text{A10})$$

which reads

$$v(k_1, k_1) = k_1^4 k_2^2 + k_1^2 k_2^4 + k_2^4 (k_1 + k_2)^2 + k_2^2 (k_1 + k_2)^4 + k_1^4 (k_1 + k_2)^2 + k_1^2 (k_1 + k_2)^4. \quad (\text{A11})$$

$H_{\text{MR}}$  can also be expressed as [3, 4]

$$H_{\text{MR}} = \frac{1024\sqrt{3}\pi^7}{L_y^8} \sum_{j_1, j_2, j_3, j_4, j_5, j_6} (j_1 - j_2)(j_1 - j_3)(j_2 - j_3)(j_6 - j_4)(j_6 - j_5)(j_5 - j_4) \delta_{j_1+j_2+j_3, j_4+j_5+j_6} \exp \left\{ -\frac{2\pi^2}{L_y^2} \left[ \sum_i j_i^2 - \frac{1}{6} \left( \sum_i j_i \right)^2 \right] \right\} c_{j_1}^\dagger c_{j_2}^\dagger c_{j_3}^\dagger c_{j_4} c_{j_5} c_{j_6} \quad (\text{A12})$$

## Appendix B: MPS representation of the ground state

For a translation invariant system, the MPS of the ground state reads

$$\Psi = \dots \text{---} \textcircled{A} \text{---} \textcircled{A} \text{---} \textcircled{A} \text{---} \dots, \quad (\text{B1})$$

where  $A$  is the local tensor defined for a unit cell. If this unit cell contains  $M$  sites, we further decompose  $A$  as a product of  $M$  local tensors defined on each site by  $A_l (l = 1, \dots, M)$ .

The Laughlin ground states are three-fold topological degenerate, corresponding to the following three initial orbital configurations (or the root partitions [5–7]):  $\{\dots 100100\dots\}$ ,  $\{\dots 010010\dots\}$ , and  $\{\dots 001001\dots\}$ . Thus, we can set  $M = 3$  and represent  $A$  as

$$\text{---} \textcircled{A} \text{---} = \text{---} \textcircled{A_1} \text{---} \textcircled{A_2} \text{---} \textcircled{A_3} \text{---} \quad (\text{B2})$$

The Laughlin state conserves the particle number and the  $y$ -axis momentum on a cylinder [8, 9]. Thus, we can assign both the particle number  $C_l$  and the momentum  $K_l$  to the vertical leg of local tensor  $A_l$ . For a given filling factor  $\nu$ ,  $(K_l, C_l)$  are defined by [8–10]

$$K_l = l(N_l - \nu), \quad (\text{Momentum}) \quad (\text{B3})$$

$$C_l = N_l - \nu, \quad (\text{Particle number}) \quad (\text{B4})$$

where  $N_l$  is the particle number at site  $l$ . Similarly, we can introduce the corresponding quantum numbers  $(\bar{K}, \bar{C})$  for each horizontal bond.

Under a translation by  $M$  sites, the physical and virtual momenta,  $K_l$  and  $\bar{K}_l$ , behave as

$$K_l \rightarrow K_l + MC_l, \quad (\text{B5})$$

$$\bar{K}_l \rightarrow \bar{K}_l + M\bar{C}_l. \quad (\text{B6})$$

This property should be taken into account in the implementation of the DMRG algorithm [9, 11, 12] and in the translation of MPS with a periodicity  $M$ .

For each local tensor, the quantum numbers satisfy the following addition rule:

$$(\bar{K}, \bar{C})_{l,\text{left}} + (K_l, C_l) - (\bar{K}, \bar{C})_{l,\text{right}} = 0 \quad (\text{B7})$$

A similar idea works for the Moore-Read (MR) state. In the even parity state, we can choose the orbital configuration  $\{\dots 10011001\dots\}$  to represent the ground state. This indicates that the minimum cell of the ground state is  $M = 4$  and

$$\text{---} \bigcirc_A \text{---} = \text{---} \bigcirc_{A_1} \text{---} \bigcirc_{A_2} \text{---} \bigcirc_{A_3} \text{---} \bigcirc_{A_4} \text{---} \cdot \quad (\text{B8})$$

In the odd-parity sector of the MR state, there are unpaired fermions. In this case, the initial orbital configuration changes from  $\{\dots 1001\dots\}$  to  $\{\dots 01\dots\}$ , and the corresponding unit cell changes from 4 to 2. Thus,  $A$  can be represented as

$$\text{---} \bigcirc_A \text{---} = \text{---} \bigcirc_{A_1} \text{---} \bigcirc_{A_2} \text{---} \cdot \quad (\text{B9})$$

In addition, a one-half quantum flux  $f = 1/2$  should attach to a local tensor in each unit cell to correctly capture the topological nature of the neutral fermion mode. Accordingly, Eq. (B7) becomes

$$(\bar{K}, \bar{C})_{l,\text{left}} + (K_l + f, C_l) - (\bar{K}, \bar{C})_{l,\text{right}} = (0, 0) \quad (\text{B10})$$

We determine all local tensors by variationally minimizing the ground state energy using the standard tensor-network methods, including the density matrix renormalization group (DMRG) and variational uniform matrix product states (VUMPS) [13]. For benchmarking, we calculate the entanglement spectrum of both the Laughlin and MR states. As shown in Fig. 1, the entanglement spectrum patterns of these two states obtained from our calculation are consistent with the published results [14].

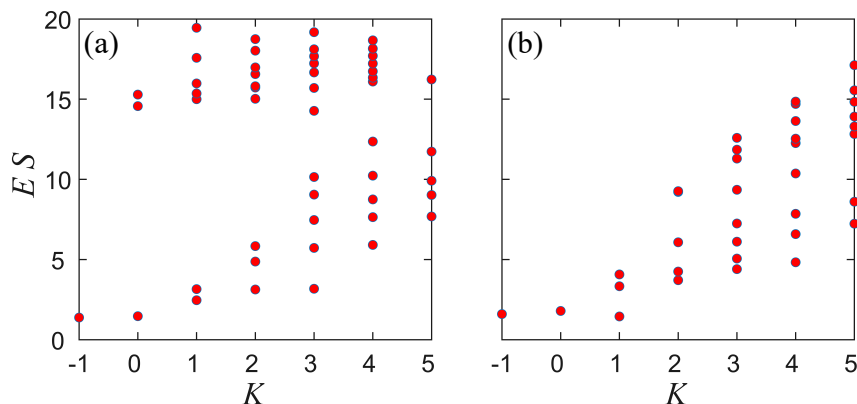


FIG. 1. Entanglement spectra of (a) the Laughlin state, the counting pattern is 1,1,2,3,5,..., and (b) the MR state, the counting pattern is 1,1,3,5,... [14].

### Appendix C: MPS representation of excited states under the single-mode approximation

Under the single-mode approximation, the excited states are represented by replacing one of the  $A$  tensors in the ground state with an impurity tensor  $B$  and then boosting into a momentum eigenstate

$$\Phi_k(B) = \sum_n e^{i\tilde{k}_x n M} \dots \text{---} \bigcirc_{A}^{n-1} \text{---} \bigcirc_B^n \text{---} \bigcirc_A^{n+1} \text{---} \dots \cdot \quad (\text{C1})$$

In this expression,  $B$  is defined on one of the unit cells. Like  $A$ , it can be further decomposed as sum of  $M$  MPS

$$\text{---} \bigcirc_B \text{---} = \text{---} \bigcirc_{B_1} \text{---} \bigcirc_{A_2} \text{---} \dots \text{---} \bigcirc_{A_M} \text{---} + \dots + e^{i\tilde{k}_x (M-1)} \text{---} \bigcirc_{A_1} \text{---} \bigcirc_{A_2} \text{---} \dots \text{---} \bigcirc_{B_M} \text{---} \cdot, \quad (\text{C2})$$



plot of  $S(k)$  on the whole  $(k_x, k_y)$  plane. Our calculation indicates that  $S(k)$  is isotropic. The peak (high intensity) positions of  $S(k)$  are consistent with previous studies [17].

- 
- [1] F. D. M. Haldane, Fractional quantization of the hall effect: A hierarchy of incompressible quantum fluid states, *Phys. Rev. Lett.* **51**, 605 (1983).
  - [2] S. A. Trugman and S. Kivelson, Exact results for the fractional quantum Hall effect with general interactions, *Phys. Rev. B* **31**, 5280 (1985).
  - [3] A. Kirmani, K. Bull, C.-Y. Hou, V. Saravanan, S. M. Saeed, Z. Papić, A. Rahmani, and P. Ghaemi, Probing geometric excitations of fractional quantum hall states on quantum computers, *Phys. Rev. Lett.* **129**, 056801 (2022).
  - [4] C. Voinea, S. Pu, A. Kirmani, P. Ghaemi, A. Rahmani, and Z. Papić, Deformed fredkin model for the  $\nu = 5/2$  moore-read state on thin cylinders, *Phys. Rev. Res.* **6**, 013105 (2024).
  - [5] B. A. Bernevig and F. D. M. Haldane, Generalized clustering conditions of jack polynomials at negative jack parameter  $\alpha$ , *Phys. Rev. B* **77**, 184502 (2008).
  - [6] B. A. Bernevig and F. D. M. Haldane, Model fractional quantum hall states and jack polynomials, *Phys. Rev. Lett.* **100**, 246802 (2008).
  - [7] B. Yang, Z.-X. Hu, Z. Papić, and F. D. M. Haldane, Model wave functions for the collective modes and the magnetoroton theory of the fractional quantum hall effect, *Phys. Rev. Lett.* **108**, 256807 (2012).
  - [8] M. P. Zaletel and R. S. K. Mong, Exact matrix product states for quantum hall wave functions, *Phys. Rev. B* **86**, 245305 (2012).
  - [9] M. P. Zaletel, R. S. K. Mong, and F. Pollmann, Topological characterization of fractional quantum hall ground states from microscopic hamiltonians, *Phys. Rev. Lett.* **110**, 236801 (2013).
  - [10] L. Hu and W. Zhu, Abelian origin of  $\nu = 2/3$  and  $2 + 2/3$  fractional quantum hall effect, *Phys. Rev. B* **105**, 165145 (2022).
  - [11] S. R. White, Density matrix formulation for quantum renormalization groups, *Phys. Rev. Lett.* **69**, 2863 (1992).
  - [12] S. R. White, Density-matrix algorithms for quantum renormalization groups, *Phys. Rev. B* **48**, 10345 (1993).
  - [13] V. Zauner-Stauber, L. Vanderstraeten, M. T. Fishman, F. Verstraete, and J. Haegeman, Variational optimization algorithms for uniform matrix product states, *Phys. Rev. B* **97**, 045145 (2018).
  - [14] H. Li and F. D. M. Haldane, Entanglement spectrum as a generalization of entanglement entropy: Identification of topological order in non-abelian fractional quantum hall effect states, *Phys. Rev. Lett.* **101**, 010504 (2008).
  - [15] L. Vanderstraeten, J. Haegeman, and F. Verstraete, Tangent-space methods for uniform matrix product states, *SciPost Phys. Lect. Notes* , 7 (2019).
  - [16] T. Xiang, *Density matrix and tensor network renormalization* (Cambridge University Press, 2023).
  - [17] J. Wang, S. D. Geraedts, E. H. Rezayi, and F. D. M. Haldane, Lattice monte carlo for quantum hall states on a torus, *Phys. Rev. B* **99**, 125123 (2019).